

# Design, Simulation and Verification of Generalized Photovoltaic cells Model Using First Principles Modeling

Atul Gupta<sup>1</sup> and Venu Uppuluri Srinivasa<sup>2</sup>

<sup>1,2</sup>Santero India Design Center, Gigaspace, Building Beta-1,  
Third floor, Office No. 301, Viman Nagar, Pune, M.H, India

<sup>1</sup>Email: atulgupta2006@gmail.com,

<sup>2</sup>Email: venuuppuluri@gmail.com

**Abstract**—This paper presents the implementation of a generalized photovoltaic model of PV cell, module, and array model applicable for mono crystalline, poly crystalline silicon, thin film like CIS, CdTe, Amorphous silicon, polymer from various manufacturers on Matlab/Simulink simulation software platform using first principle method. This model is known to have better accuracy estimation of electrical behavior of the cell with respect to changes on environmental parameter of temperature and irradiance. All inputs to the model can be easily extracted from standard PV module datasheet. The functioning of the proposed model is evaluated by simulation. The accuracy of the simulation is verified by comparing output current and power characteristics of PV cell with datasheet provided by PV cell manufacturers.

**Index Terms**— pv modeling, mono-crystalline, multi-crystalline, pv module, STC, thin-film, matlab, simulink

## I. INTRODUCTION

Recently, PV systems have received a great deal of attention due to the exhaustion of energy sources, high oil prices and environmental pollution. The World Energy Forum has predicted that fossil based oil, coal and gas reserves will be exhausted in less than another 10 decades. Fossil fuels account for over 79% of the primary energy consumed in the world, and 57.7% of that amount is used in the transport sector and are diminishing rapidly. This results in 40% of carbon footprint across the globe.

The amount of incoming solar energy in one year is equivalent to fifty times the known reserves of coal, 800 times the known oil reserves. A PV system directly converts solar energy into electric energy. A powerful attraction of PV systems is that they produce electric power without harming the environment, by directly transforming a free inexhaustible source of energy, solar radiation, into electricity. This fact, together with the continuing decrease in PV arrays cost (tenfold in the last two decades) and the increase in their efficiency (threefold over the same period). Commercial Photovoltaic cells were first developed in Bell lab in 1954 with 6% efficiency. But, only after their use in space programs in 1950's commercial interest surged up. Since then interest in their use in various applications like power supplies to residential appliances, grid connected solar inverter, telecommunications, refrigeration and water pumping.

In PV power generation, due to the high cost of modules, optimal utilization of the available solar energy has to be ensured. Also PV system requires special design considerations due to the varying nature of the solar power resulting from unpredictable and sudden changes in weather conditions, which change the radiation level as well as the cell operating temperature. This mandates an accurate and reliable simulation of designed PV systems prior to installation.

## II. PHOTOVOLTAIC CELL

Solar cells consist of a p-n junction fabricated in a thin wafer or layer of semiconductor. In the dark, the I-V output characteristic of a solar cell has an exponential characteristic similar to that of a diode.

When exposed to light, photons with energy greater than the bandgap energy ' $E_g$ ' of the semiconductor are absorbed and create an electron-hole pair. These carriers are swept apart under the influence of the internal electric fields of the p-n junction and create a current proportional to the incident radiation. When the cell is short circuited, this current flows in the external circuit; when open circuited, this current is shunted internally by the intrinsic p-n junction diode. The characteristics of this diode therefore set the open circuit voltage characteristics of the cell.

## III. MODELLING THE SOLAR CELL

The simplest equivalent circuit of a solar cell is an ideal current source in parallel with a diode [1-4]. The current source represents the current generated by photons (often denoted as  $I_{ph}$ ), and its output is constant under constant temperature and constant incident radiation of light. The diode determines the I-V characteristics of the cell.

Increasing sophistication, accuracy and complexity can be introduced to the model by adding in turn.

- Temperature dependence of the diode saturation current.
- Saturation current contribution due to diffusion process.
- Saturation current contribution due to recombination in the space charge layer effect dominant at higher bias region.

- In small size solar cells leakage current has an effect on the low bias region.
- Temperature dependence of the photo current  $I_{ph}$ .
- Shunt resistance  $R_p$  in parallel with the diode [11-15].
- Series resistance  $R_s$ , which gives a more accurate shape between the maximum power point and the open circuit voltage [5-10].
- Either allowing the diode quality factor  $A$  to become a variable parameter (instead of being fixed at either 1 or 2) or introducing two parallel diodes (one with  $A = 1$ , one with  $A = 2$ ) with independently set saturation currents.

The single exponential model or the double exponential model usually represents the PV panel. The single and the double exponential model are shown in Fig. 1 and 2 respectively. The current is expressed in terms of voltage, current and temperature as shown in (1).

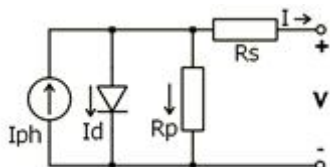


Figure 1. Single exponential model of a PV Cell

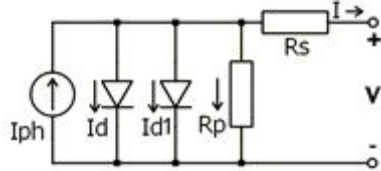


Figure 2. Double exponential model of PV Cell

For this research work, three different types of model starting from simplicity to complexity were used.

Type1: Single diode model with  $R_s$  neglecting  $R_p$ .

Type2: Single diode model with  $R_s$  and  $R_p$ .

Type3: Complex Double diode model with  $R_s$  and  $R_p$

#### A. Current-Voltage I-V Curve for a Solar Cell

Fig. 3 shows the I-V characteristic curve of a solar cell for certain irradiance 'G' at a fixed cell temperature 'T'. The current from a PV cell depends on the external voltage applied and the amount of sunlight on the cell. When the cell is short-circuited, the current is at maximum (short-circuit current ' $I_{sc}$ '), and the voltage across the cell in open circuit condition is at its maximum (open circuit voltage ' $V_{oc}$ '), and the current is '0'.

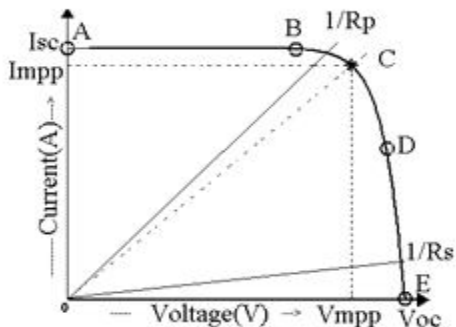


Figure 3. A typical Current voltage I-V curve for photovoltaic cells

If the cell's terminals are connected to a variable resistance,  $R$ , the operating point is determined by the intersection of the  $I$ - $V$  characteristic of the solar cell with the load  $I$ - $V$  characteristics. As shown in Fig. 3 for a resistive load, the load characteristic is a straight line with a slope  $I/V = 1/R$ . If the load resistance is small, the cell operates in the region  $AB$  of the curve, where the cell behaves as a constant current source, almost equal to the short circuit current. On the other hand, if the load resistance is large, the cell operates on the region  $DE$  of the curve, where the cell behaves more as a constant voltage source, almost equal to the open circuit voltage [16]. Point  $C$  on Fig. 3 is also called the maximum power point, which is the operating point ( $P_{max}$ ) at which the output power is maximized. The model included temperature dependence of the photocurrent  $I_{ph}$  and the saturation current of the diode  $I_o$ . Diode quality factor 'A' set to achieve the best curve match. The circuit diagram for the solar cell is shown in Fig. 1 and 2.

#### B. Type-1 PV Model

The equations, which describe the I-V characteristics of Type1, are

$$I = I_{ph} - I_o \left[ \exp\left(\frac{q(V + IR_s)}{AkT}\right) - 1 \right] \quad (1)$$

where,  $I$  is the PV array output current (A);  $V$  is the PV array output voltage (V);  $q$  is the charge of an electron;  $k$  is Boltzmann's constant;  $A$  is the p-n junction quality/ideality factor;  $T$  is the cell temperature (K); and  $I_o$  is the cell reverse saturation current. The factor 'A' in (1) determines the cell deviation from the ideal p-n junction characteristics; it ranges between 1 and 2, 1 being the ideal value.

The value of  $R_s$  was calculated by evaluating the slope  $dI/dV$  of the I-V curve at the  $V_{oc}$ . The equation for  $R_s$  was derived by differentiating the I-V equation and then rearranging it in terms of  $R_s$  [17-18].

$$R_s = - \left| \frac{dV}{dI} \right|_{V_{oc}} - \frac{1}{q \cdot I_o \exp\left(\frac{qV_{oc}}{AkT}\right)} \quad (2)$$

Where,  $dV/dI$  is the slope of the I-V curve at the  $V_{oc}$ . The cell reverse saturation current  $I_o$  varies with temperature according to the following equation [19-20].

$$I_o = I_{or} \left[ \frac{T}{T_r} \right]^{\frac{3}{A}} \exp\left(\frac{qE_g}{Ak} \left[ \frac{1}{T_r} - \frac{1}{T} \right]\right) \quad (3)$$

where,  $T_r$  is the cell reference temperature,  $I_{or}$  is the reverse saturation current at  $T_r$  and  $E_g$  is the band-gap energy of the semiconductor used in the cell. The photocurrent  $I_{ph}$  depends on the solar radiation and the cell temperature as follows:

At the open circuit point on the I-V curve,  $V=V_{oc}$ ,  $I=0$ . Also at short circuit point on the I-V curve  $I_{ph}=I_{sc}$ . After substituting these values in (1) the expression for  $I_o$  at STC

can be obtained.

$$I_{or} = \frac{I_{scr}}{\exp\left(\frac{q \cdot V_{ocr}}{AkT_r}\right) - \exp\left(\frac{q \cdot I_{scr} R_s}{AkT_r}\right)} \quad (4)$$

Where,  $I_{scr}$ ,  $V_{ocr}$  are given in the datasheet at STC. The  $I_{sc}$  is proportional to the intensity of irradiance, thus  $I_{ph}$  at subjected G and T is given by

$$I_{sc} = I_{scr} \cdot \left[1 + K_i \cdot \left(T - T_r\right)\right] \cdot \frac{G}{1000}. \quad (5)$$

Where,  $K_i$  is the temperature coefficient of  $I_{sc}$  in percent change per degree temperature also given in the datasheet. Since  $I_o$  varies with temperature thus can be calculated from (3). Similarly  $I_{sc}$  from (5).  $I_{ph}$  at subjected G and T is given by

$$I_{ph} = I_{sc} + I_o \left[ \exp\left(\frac{q \cdot I_{sc} R_s}{AkT}\right) - 1 \right]. \quad (6)$$

The PV array power  $P$  can be calculated using (1) as follows:

$$P = IV = I_{ph}V - I_oV \left[ \exp\left(\frac{q \cdot (V + IR_s)}{AkT}\right) - 1 \right] \quad (7)$$

From which the MPOP voltage  $V_{mpp}$  can be calculated by setting  $dP/dV = 0$ ; thus at the MPOP

$$\frac{dP}{dV} = \exp\left(\frac{q \cdot (V_{mpp} + I_{ph}R_s)}{AkT}\right) \cdot \left[ \left( \frac{qV_{mpp}}{AkT} \right) + 1 \right] - \frac{I_{ph} + I_o}{I_o} = 0. \quad (8)$$

Approximate value of A at STC on MPOP is given by

$$\frac{\exp\left(\frac{q \cdot (V_{mppr} + I_{mppr}R_s)}{AkT_r}\right) - \exp\left(\frac{q \cdot I_{scr}R_s}{AkT_r}\right)}{\exp\left(\frac{q \cdot V_{ocr}}{AkT_r}\right) - \exp\left(\frac{q \cdot I_{scr}R_s}{AkT_r}\right)} = \frac{I_{scr} - I_{mppr}}{I_{scr}}. \quad (9)$$

$V_{mppr}$ ,  $I_{mppr}$  and  $I_{scr}$  is given in datasheet of PV cells/Panel. Solving (8) and (9) using numerical methods,  $V_{mpp}$  and A can be calculated.

Finally, the equation of  $I-V$  characteristics was solved using the Newton's method for rapid convergence of the answer, because the solution of current is recursive by inclusion of a series resistance in the model [21]. The Newton's method is described as:

$$x_{n+1} = x_n - \frac{f(x_n)}{f'(x_n)} \quad (10)$$

Where:  $f'(x)$  is the derivative of the function,  $f(x) = 0$ ,  $x_n$  is a present value and  $x_{n+1}$  is a next value.

$$f(I) = -I + I_{ph} - I_o \left\{ \exp\left(\frac{q \cdot (V + IR_s)}{AkT}\right) - 1 \right\} = 0 \quad (11)$$

By using the above equations the following output current ( $I$ ) is computed iteratively.

$$I_{n+1} = I_n - \frac{I_{ph} - I_n - I_o \left\{ \exp\left(\frac{q \cdot (V + IR_s)}{AkT}\right) - 1 \right\}}{-1 - I_o \left( \frac{q \cdot R_s}{AkT} \right) \left\{ \exp\left(\frac{q \cdot (V + IR_s)}{AkT}\right) \right\}} \quad (12)$$

By making step variations in the solar radiation 'G' and the cell temperature 'T' in (1-4), the I-V characteristics of the PV array can be simulated as shown in Fig. 4 and 5. Simulation of the PV array provides a flexible means of analyzing and comparing the MPOP when operated under randomly varying solar radiation and cell temperature. All of the constants in the above equations can be determined by examining the manufacturers ratings of the PV array, and then the published or measured I-V curves of the array. As a typical example, the Sunpower A300 was used to illustrate and verify the model.

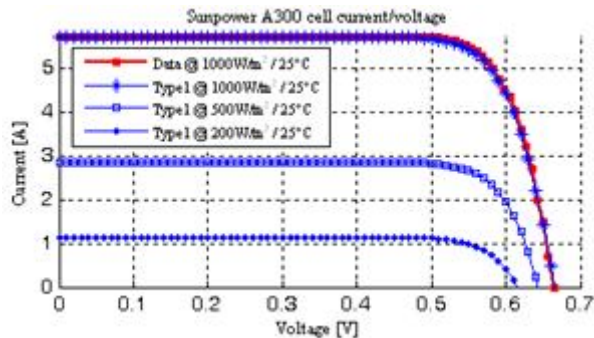


Figure 4. I-V curves of SunpowerA300Cell at various irradiance

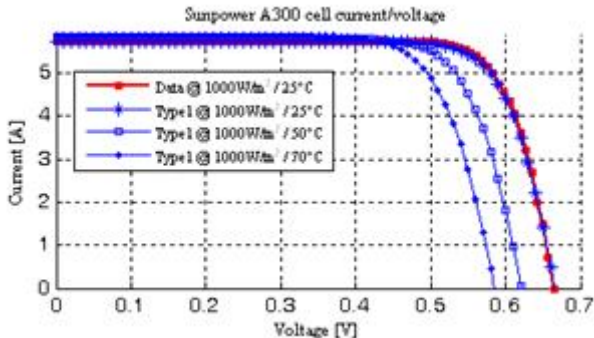


Figure 5. I-V curves of SunpowerA300Cell at various Temperatures  
The open circuit voltage corresponds to the voltage drop across the diode when it was traversed by the photocurrent  $I_{ph}$ , which is equal to  $I_{sc}$ , when the generated current is  $I=0$ . It can be solved for  $V_{oc}$

$$V_{oc} = \frac{AkT_r}{q} \ln \left( \frac{I_{ph}}{I_o} + 1 \right) = V_t \ln \left( \frac{I_{ph}}{I_o} + 1 \right) \quad (13)$$

Where,  $V_t$  – thermal voltage (V)

Change of cell temperature with ambient temperature can be expressed by the following linearity

$$T_a = T_o + \frac{(NOCT - 20)}{800} G. \quad (14)$$

Solar radiation was the first and temperature was the second most important effect. So, this study examined these important effecting parameters. Typically voltage decreases with increasing temperature, and current increases (although slightly), the combined effect being that power decreases. For instance; a polycrystalline module operating typically at 45 °C will therefore produce roughly 10% less power than predicted by its nominal standard test conditions rating. The series resistance ( $R_s$ ) of the PV module has a large impact on the slope of the  $I-V$  curve near the open-circuit voltage ( $V_{oc}$ ),

### C. Type-2 PV Model

The equations, which describe the  $I-V$  characteristics of the cell modeled for Type-3, are

$$I = I_{ph} - I_o \left\{ \exp \left[ \frac{q \cdot (V + IR_s)}{AkT} \right] - 1 \right\} - \frac{V + IR_s}{R_p}. \quad (15)$$

$R_s$  has a very marked effect upon the slope of the  $I-V$  curve at  $V=V_{oc}$ . The value of  $R_s$  was calculated by evaluating the slope  $dI/dV$  of the  $I-V$  curve at the  $V_{oc}$ . The equation for  $R_s$  was derived by differentiating the  $I-V$  equation and then rearranging it in terms of  $R_s$  in (15).

$$R_s = - \left| \frac{dV}{dI} \right|_{V_{oc}} - \frac{\frac{R_s}{R_p}}{\frac{1}{\frac{q \cdot I_o}{AkT} \exp \left( \frac{qV_{oc}}{AkT} \right) + \frac{1}{R_p}}} \quad (16)$$

Examination of (16) shows that in the adjacent of  $V_{oc}$  the  $1/R_p$  may be neglecting. Therefore the final equation for  $R_s$  is same as (2).  $R_p$ , however, has an effect upon the lateral position of the MPP together with a less marked effect upon the slope of the curve at  $V=0$ ,  $I=I_{sc}$ . The value of  $R_p$  is calculated by evaluating the slope  $dI/dV$  of the  $I-V$  curve at the  $I_{sc}$ . The equation for  $R_p$  is derived by differentiating the  $I-V$  equation and then rearranging it in terms of  $R_p$  in (16).

$$R_p = - \frac{1}{\left( \left| \frac{dV}{dI} \right|_{I_{sc}} + R_s \right) + \frac{q \cdot I_o}{AkT} \exp \left( \frac{q \cdot I_{sc} R_s}{AkT} \right)} \quad (17)$$

At the open circuit point on the IV curve,  $V=V_{oc}$ ,  $I=0$ . Also at short circuit point on the IV curve  $I_{ph}=I_{sc}$ . After substituting these values in the (15) the expression for  $I_o$  at STC can be obtained.

$$I_{or} = \frac{I_{scr} - \frac{V_{oc} - I_{scr} R_s}{R_p}}{\exp \left( \frac{q \cdot V_{oc}}{AkT_r} \right) - \exp \left( \frac{q \cdot I_{scr} R_s}{AkT_r} \right)} \quad (18)$$

Since  $I_o$  varies with temperature thus can be calculated from (3). Similarly  $I_{sc}$  from (5).  $I_{ph}$  at subjected G and T is given by

$$I_{ph} = I_{sc} + I_o \left[ \exp \left( \frac{q \cdot I_{sc} R_s}{AkT} \right) - 1 \right] + \frac{I_{sc} R_s}{R_p}. \quad (19)$$

The PV array power  $P$  can be calculated using (15) as follows:

$$P = IV = I_{ph} V - I_o V \left[ \exp \left( \frac{q \cdot (V + IR_s)}{AkT} \right) - 1 \right] \quad (20)$$

From which the MPOP voltage  $V_{mpp}$  can be calculated by setting  $dP/dV=0$ ; thus at the MPOP

$$\frac{dP}{dV} = \exp \left( \frac{q \cdot (V_{mpp} + I_{ph} R_s)}{AkT} \right) \cdot \left[ \left( \frac{qV_{mpp}}{AkT} \right) + 1 \right] + \frac{2 \cdot V_{mpp} + I_{ph} R_s}{I_o R_p} - \frac{I_{ph} + I_o}{I_o} = 0 \quad (21)$$

Approximate value of A at STC on MPOP is given by

$$\frac{\exp \left( \frac{q \cdot (V_{mpp} + I_{mpp} R_s)}{AkT_r} \right) - \exp \left( \frac{qI_{scr} R_s}{AkT_r} \right)}{\exp \left( \frac{qV_{oc}}{AkT_r} \right) - \exp \left( \frac{qI_{scr} R_s}{AkT_r} \right)} = \frac{I_{scr} - I_{mpp} + \frac{I_{scr} R_s}{R_p} - \frac{V_{mpp} - I_{mpp} R_s}{R_p}}{I_{scr} - \frac{V_{oc} + I_{scr} R_s}{R_p}} \quad (22)$$

$V_{mpp}$ ,  $I_{mpp}$  and  $I_{scr}$  is given in datasheet of PV cells/Panel. Solving (21) and (22) using numerical methods,  $V_{mpp}$  and A can be calculated.

From (10), current ( $I$ ) is computed iteratively.

$$I_{n+1} = I_n - \frac{I_{ph} - I_n - I_o \left\{ \exp \left[ \frac{q \cdot (V + IR_s)}{AkT} \right] - 1 \right\} - \frac{V + IR_s}{R_p}}{-1 - I_o \left( \frac{q \cdot R_s}{AkT} \right) \left\{ \exp \left[ \frac{q \cdot (V + IR_s)}{AkT} \right] - \frac{R_s}{R_p} \right\}} \quad (23)$$

### D. Type 3 PV Model

The single diode models were based on the assumption that the recombination loss in the depletion region is absent. In a real solar cell, the recombination represents a substantial loss, especially at low voltages. This cannot be adequately modeled using a single diode.

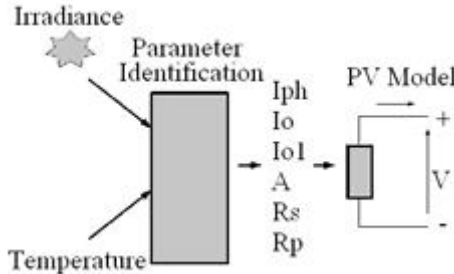


Figure 6. Modeling of Double diode PV cell

Consideration of this loss leads to a more precise model known as the two-diode model [22-25]. The equation, which describe the I-V characteristics of the cell modeled for Type 3, is

$$I = I_{ph} - I_{or} \left\{ \exp \left[ \frac{q(V + IR_s)}{AKT} \right] - 1 \right\} - I_{or1} \left\{ \exp \left[ \frac{q(V + IR_s)}{AKT} \right] - 1 \right\} - \frac{V + IR_s}{R_p} \quad (24)$$

Where,  $I_{ph}$ : the photo generated current;  $I_o$ : the dark saturation current;  $I_{or}$ : saturation current due to diffusion;  $I_{or1}$ : is the saturation current due to recombination in the space charge layer;  $I_{Rp}$ : current flowing in the shunt resistance;  $R_s$ : cell series resistance;  $R_p$ : the cell (shunt) resistance.

Furthermore, the parameters ( $I_{ph}$ ,  $I_o$ ,  $I_{or1}$ ,  $R_s$ ,  $R_{sh}$  and  $A$ ) vary with temperature, irradiance and depend on manufacturing tolerance as shown in Fig. 6. Numerical methods and curve fitting can also be used to estimate them [26-30].

#### IV. SIMULATION RESULT

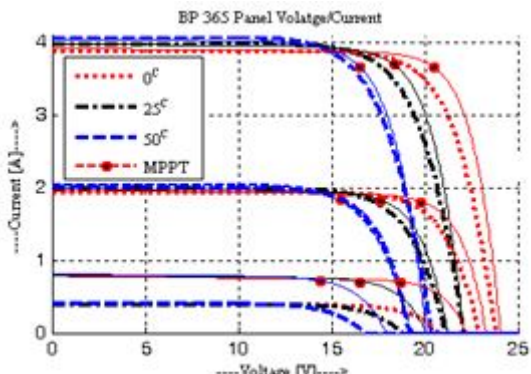


Figure 7. I-V curves for BP365 modules at different 'G' and 'T'

TABLE I. PARAMETERS FOR THE PROPOSED MODELS

Parameter at STC	Mono-Crystalline		m-Si BP365	CIGS PAE SE15
	SPA300	SPA318		
P <sub>max</sub> (W)	3	318	65	15
I <sub>sc</sub> (A)	5.75	6.20	3.99	1.05
V <sub>oc</sub> (V)	0.665	64.7	21.1	28
I <sub>app</sub> (A)	5.35	5.82	3.69	0.81
V <sub>app</sub> (V)	0.560	54.7	17.6	18.56
K <sub>v</sub> (mV/°C)	-1.9	-176.6	-80	-168
K <sub>p</sub> (% / °C)	-0.38	-0.38	-0.5	-0.66
K <sub>i</sub> (mA / °C)	3.5	3.5	2.59	0.168
NOCT (°C)	45±2	45±2	47±2	44.5
N <sub>s</sub>	--	96	36	48

TABLE II. PARAMETERS USED IN MODELS

Parameter	Mono-Crystalline A300			Mono-Crystalline A318		
	T-1	T-2	T-3	T-1	T-2	T-3
R <sub>s</sub> (Ω)	0.015	0.015	0.015	5.4	5.4	5.4
R <sub>p</sub> (Ω)	--	300	300	--	11400	11400
A	1.2	1.2	1	1.2	1.2	1
A <sub>t</sub>	--	--	2	--	--	2
I <sub>er</sub> (A)	4e-10	4e-10	4e-10	--	--	4e-10
I <sub>er1</sub> (A)	--	--	4e-10	--	--	4e-10
E <sub>g</sub> (eV)	1.12	1.12	1.12	1.12	1.12	1.12

TABLE III. PARAMETERS USED IN MODELS

Parameter	Multi-Crystalline			Thin-Film		
	T-1	T-2	T-3	T-1	T-2	T-3
R <sub>s</sub> (Ω)	0.1	0.1	0.1	10	10	10
R <sub>p</sub> (Ω)	--	400	400	--	380	380
A	1.3	--	1	1.5	1.5	1
A <sub>t</sub>	--	--	2	--	--	2
I <sub>er</sub> (A)	8e-10	6e-10	6e-10	9e-10	9e-10	9e-10
I <sub>er1</sub> (A)	--	--	6e-10	--	--	9e-10
E <sub>g</sub> (eV)	1.14	1.14	1.14	1.38	1.38	1.38

The two diode model described in this paper was validated by the measured parameters of selected PV modules. Four modules of different brands/models were utilized for verification; these include the multi- and mono-crystalline as well as the thin-film types. The specifications of the modules are summarized in Table I. The computational results are compared with the  $R_s$  and  $R_p$  models. Note that these two models are shown in Fig. 1 and 2, respectively. Table II. and III. shows the parameters of the proposed two-diode model. Fig. 7 shows the I-V curves for BP365 modules at different G (0.2,0.5 and 1kW/m<sup>2</sup>) and T(0,25 and 50°C)

#### V. PHOTOVOLTAIC MODULE MODELING

Module is generally consisting of series and parallel combination of PV cells. Once the I-V or P-V characteristics of individual cells are known then it can easily calculated for whole module [31-33]. As shown in Fig. 8.

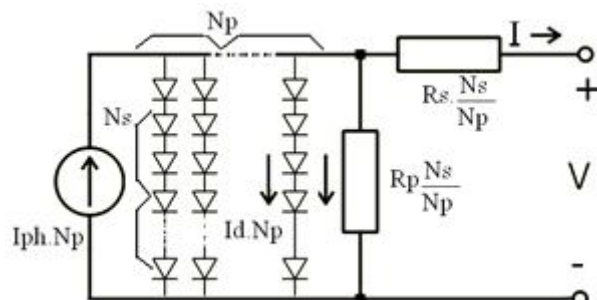


Figure 8. Module consist of series parallel combination of cells

#### CONCLUSIONS

In this paper, a MATLAB Simulink PV system simulator based on an improved two-diode model is proposed. To reduce the computational time, the input parameters were reduced to four and the values of  $R_p$  and  $R_s$  were estimated by an efficient iteration method. The general model was implemented on MATLAB script file, and accepts irradiance and temperature as variable parameters and outputs the I-V characteristic. Furthermore the input information to simulator

was available on standard PV module datasheets. The simulation of large array can be interfaced with MPPT algorithm in digital domain [34]. The accurateness of the simulator is verified with four PV modules of different types (multi-crystalline, mono-crystalline and thin-film) from various manufacturers. It is observed that the two-diode model is superior to the Rp and Rs models. The results are found to be in close agreement with the theoretical predictions.

## APPENDIX

I&V	Cell output current and voltage
AM	Air Mass ratio
$I_{ph}$	Photon or light generated current
$I_o$	PN junction saturation current
q	Electronic charge
A	Ideality factor
k	Boltzman's constant
$R_s$	Series resistance
$R_p$	Shunt resistance
T	Operating cell temperature
$I_{sc}$	Short circuit current at STC
$K_i$	Short ckt. current temperature coefficient at ISCR
G	Solar Insolation in $\text{W/m}^2$ .
STC	Standered Test Condition, T=25, AM=1.5, G=1
Tr	Reference temperature at STC
Eg	Forbidden gap
FF	Fill Factor
$N_p$	No. of parallel connected cells
$N_s$	No. of series connected cells
NOCT	Normal operating cell temperature.
MPOP	Maximum power operating point

## REFERENCES

- [1] M. C. Glass, "Improved solar array power point model with SPICE realization," in Proc. IECEC, Vol. 1, pp. 286–291, Aug. 1996.
- [2] Y. T. Tan, D. S. Kirschen, and N. Jenkins, "A model of PV generation suitable for stability analysis," IEEE Trans. Energy Convers., Vol. 19, No. 4, pp. 748–755, Dec. 2004.
- [3] A. Kajihara and A. T. Harakawa, "Model of photovoltaic cell circuits under partial shading," in Proc. ICIT, pp. 866–870, 2005.
- [4] N. D. Benavides and P. L. Chapman, "Modeling the effect of voltage ripple on the power output of photovoltaic modules," IEEE Trans. Ind. Electron., Vol. 55, No. 7, pp. 2638–2643, Jul. 2008.
- [5] W. Xiao, W. G. Dunford, and A. Capel, "A novel modeling method for photovoltaic cells," in Proc. PESC, Vol. 3, pp. 1950–1956, 2004.
- [6] G. Walker, "Evaluating MPPT converter topologies using a matlab PV model," J. Elect. Electron. Eng., Vol. 21, No. 1, pp. 45–55, 2001.
- [7] F. González-Longatt, Model of photovoltaic module in MatlabTM, II CIBELEC, 2005.
- [8] N. Celik and N. Acikgoz, "Modelling and experimental verification of the operating current of mono-crystalline photovoltaic modules using four- and five-parameter models," Applied Energy, Vol. 84, No. 1, pp. 1–15, Jan. 2007.
- [9] Y. C. Kuo, T.-J. Liang, and J.-F. Chen, "Novel maximum-power-point tracking controller for photovoltaic energy conversion system," IEEE Trans. Ind. Electron., Vol. 48, No. 3, pp. 594–601, Jun. 2001.
- [10] Y. Yusof, S. H. Sayuti, M. Abdul Latif, and M. Z. C. Wanik, "Modeling and simulation of maximum power point tracker for photovoltaic system," in Proc. PEC, pp. 88–93, 2004.
- [11] C. Carrero, J. Amador, and S. Arnaltes, "A single procedure for helping PV designers to select silicon PV module and evaluate the loss resistances," Renewable Energy, Vol. 32, No. 15, pp. 2579–2589, Dec. 2007.
- [12] S. Liu and R. A. Dougal, "Dynamic multiphysics model for solar array," IEEE Trans. Energy Convers., Vol. 17, No. 2, pp. 285–294, Jun. 2002.
- [13] S. Yadir, M. Benhmida, M. Sidki, E. Assaid, and M. Khaidar, "New method for extracting the model physical parameters of solar cell using explicit analytic solutions of current-voltage equation," in Proc. ICM, pp. 390–393, 2009.
- [14] S. Aazou and E. M. Assaid, "Modeling real photovoltaic solar cell using Maple," in Proc. ICM, pp. 394–397, 2009.
- [15] M. G. Villalva, J. R. Gazoli, and E. R. Filho, "Comprehensive approach to modeling and simulation of photovoltaic arrays," IEEE Trans. Power Electron., Vol. 24, No. 5, pp. 1198–1208, May 2009.
- [16] A. Hansen, P. Lars, H. Hansen and H. Bindner, "Models for a Stand-Alone PV System". Risø National Laboratory, Roskilde, December2000, ISBN 87-550-2776-8.
- [17] J. A. Gow and C. D. Manning, "Development of a photovoltaic array model for use in power-electronics simulation studies," IEE Proc. Elect. Power Appl., Vol. 146, No. 2, pp. 193–200, 1999.
- [18] J. A. Gow and C. D. Manning, "Development of a model for photovoltaic arrays suitable for use in simulation studies of solar energy conversion systems," in Proc. 6th Int. Conf. Power Electron. Variable Speed Drives, pp. 69–74, 1996.
- [19] Walker, Geoff R. "Evaluating MPPT converter topologies using a MATLAB PV model" Australasian Universities Power Engineering Conference, AUPEC '00, Brisbane, 2000.
- [20] Adel El Shahat, "PV cell module modeling & ANN simulation for smart grid applications," Journal of Theoretical and Applied Information Technology, pp. 13.
- [21] F.M. Gonzalez-Longatt, "Model of photovoltaic module in matlab," 2nd Latin American Congress of Students of Electrical Engineering 2005, pp. 3
- [22] C. Sah, R. N. Noyce, and W. Shockley, "Carrier generation and recombination in p-n junctions and p-n junction characteristics," in Proc. IRE, Vol. 45, No. 9, pp. 1228–1243, 1957.
- [23] J. Hyvarinen and J. Karila, "New analysis method for crystalline siliconcells," in Proc. WCPEC, Vol. 2, pp. 1521–1524, 2003.
- [24] K. Kurobe and H. Matsunami, "New two-diode model for detailed analysis of multicrystalline silicon solar cells," Jpn. J. Appl. Phys., Vol. 44, pp. 8314–8321, Dec. 2005.
- [25] K. Nishioka, N. Sakitani, K. Kurobe, Y. Yamamoto, Y. Ishikawa, Y. Uraoka, and T. Fuyuki, "Analysis of the temperature characteristics in polycrystalline si solar cells using modified equivalent circuit model," Jpn. J. Appl. Phys., Vol. 42, pp. 7175–7179, Dec. 2003.
- [26] K. Ishaque, Z. Salam and H Taheri, "Accurate MATLAB simulink PV system simulator based on a two-diode model", JPE 11-2-9, pp. 179–183.
- [27] A. Hovinen, "Fitting of the Solar Cell /V-curve to the Two Diode Model," Physica Scripta, Vol. T54, pp. 175–176, Jun. 1994.
- [28] Matlab and Simulink, The Mathworks, Inc. as of September 2011, <http://www.mathworks.com>.
- [29] Ali Keyhani, Mohammad N. Marwali, and Min Dai, "Integration of Green and Renewable Energy in Electric Power

Systems," Wiley, January 2010.

[30] Masters, Gilbert M. Renewable and Efficient Electric Power Systems John Wiley & Sons Ltd, 2004.

[31] D. Archer and R. Hill, "Clean electricity from photovoltaics, Series on Photoconversion of Solar Energy," Imperial College Press, pp. 868, Jun. 2001

[32] S. Chowdhury, G. A. Taylor, S. P. Chowdhury, A. K. Saha, and Y. H. Song, "Modelling, simulation and performance analysis of a PV array in an embedded environment," in Proc. UPEC, pp. 781–785, 2007.

[33] Atul Gupta, Ankit Soni and Venu Uppuluri Srinivasa, "Generalized Accurate Modeling of various PV Cells/Module using MATLAB Simulink", Short listed in Electronics & Engineering conference of CEE(2011), ACEEE.

[34] Atul Gupta, Amita Chandra, "Fully digital controlled front-end converter based on boost topology", pp. 171—176, CCPE (2010), ACEEE.



**Atul Gupta** received the B.E. degree in electronics and telecom engineering from Army Institute of Technology, affiliated to Pune University, MH, India, in 2002, and the M.Tech. degree in instrumentation from School Of Instrumentation, affiliated to DAVV University, Indore, MP, India. From 2004 to 2007, he was with the Research Division, TVS Electronics, Bangalore,

India, where he was working on development of On-Line uninterruptible power system, sine wave inverters, and low-power dc–dc converters. He also worked at Emerson Network Power as Champion R&D at head office at thane, India. Since Sept 2007, he has been with the India Engineering Design Center, Carraro Technologies, Pune, India, working on grid connected advance solar inverter design. His research interest includes power conditioning, Solar Energy, Hybrid Energy; Grid Interconnection of Renewable Energy sources.



**Venu Uppuluri Srinivasa**, holds Master's degree in Mechanical from Osmania University, Hyderabad, A.P, India. He also holds Master's degree in management & Post graduate diploma in Financial Management discipline. Has over 20 years of experience as an IT / ITes Technologist with both established public companies and Venture funded startups. Held senior executive roles in product marketing, strategy, product development and business development. Currently working as General Manager and Head for Carraro Technologies India Limited (an Italian Company) since 6 years representing Board as an authorized signatory. Also signed as board of director for Santerno India Private Limited. Served in the capacity of Engineering Director for Emerson Electric Co. (USA), Group Manager for Tecumseh Products India Limited etc.